




Dielectric, ferroelectric and magnetoelectric investigations of SrFe₁₂O₁₉-embedded PVDF-HFP nanocomposite fiber mats for flexible electronic applications

Sobi K. Chacko¹ and B. Raneesh^{1,*} 

¹Department of Physics, Catholicate College, Pathanamthitta, Kerala 689 645, India

Received: 9 September 2022

Accepted: 13 December 2022

Published online:
6 January 2023

© The Author(s), under exclusive licence to Springer Science+Business Media, LLC, part of Springer Nature 2023

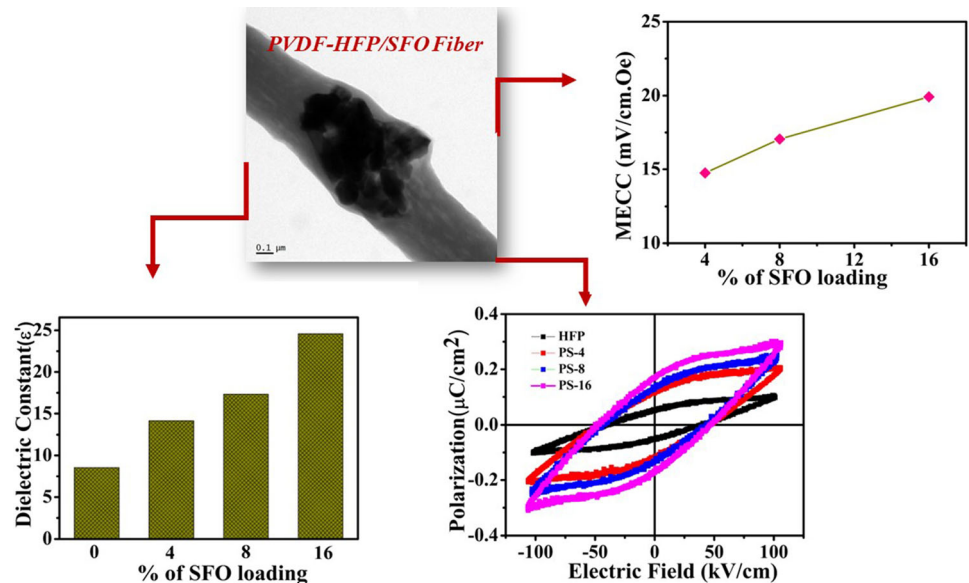
ABSTRACT

Magnetoelectric (ME) materials are capable of use in multifunctional devices due to their eccentric properties. Flexibility is a beneficial trait for enabling ME materials to be utilized in advanced device fabrication. We introduced varying weight percentages (4, 8, 16 wt%) of magnetostrictive SrFe₁₂O₁₉ (SFO) nanoparticles into a piezoelectric PVDF-HFP to fabricate flexible magnetoelectric nanocomposite fibers. Structural and morphological modifications of the composite fiber mats were investigated using X-ray diffraction (XRD), Fourier-Transform Infrared Spectroscopy (FTIR), Field Emission Scanning Electron Microscopy (FESEM), and Transmission Electron Microscopy (TEM) analysis. Dielectric and Ferroelectric studies were conducted and an exceptional enhancement in the dielectric constant and ferroelectric parameters was observed for 16% of SFO loaded sample. The magnetoelectric coupling coefficient (MECC) improved to 19.9 mV/cm. Oe for the higher filler-loaded composite sample. Additionally, mechanical studies were also done to ensure the flexibility of the composite fiber mats.

Handling Editor: Kevin Jones.

Address correspondence to E-mail: raneesh.b@gmail.com; raneesh.b@catholicatecollege.ac.in

GRAPHICAL ABSTRACT



Introduction

Developing composite multiferroic materials, exhibiting multifunctional properties and magneto-electric properties, gained much attention in the last decades. The phenomenon of coupling between the magnetic and ferroelectric orderings and the possibility of tuning the polarization by an external magnetic field and vice versa opened new possibilities and compatibility in various applications [1–5]. Composite multiferroic materials exhibit better electrical, thermal, and magnetoelectrical properties than many of the single-phase multiferroic materials [3, 6]. The organic–inorganic multiferroic composite structures help achieve higher flexibility along with remarkable multiferroic nature, which is a necessary factor in the fabrication of next-generation electronic devices [7]. The outcome of the composite is a combination of the properties of the individual components. Therefore, the selection of the polymer, which contributes to the ferroelectric characteristics, and the filler, which contributes to the magnetic/magnetostrictive nature plays a crucial role in defining the outcome of the composite.

PVDF and its copolymers are widely used electroactive polymers in the fabrication of polymer-based multiferroic materials due to their superior piezoelectric response, dielectric constant higher hydrophobicity, mechanical strength, chemical and thermal stability, etc. [7–9] PVDF is also explored as a promising candidate of polymer electrolytes [10]. PVDF and its copolymers exist in five different phase forms α , β , γ , δ , and ϵ . [9, 11] α is the commonly occurring form that can be converted into polar forms by suitable fabrication methods. Polar- β and semi-polar γ phases contribute higher electroactive nature to the PVDF matrix. The extent of the ferroelectric nature in the polymer is determined by the fraction of polar phases present in it. [9, 11]

Among the various fabrication methods used to process enhanced electroactive phase in PVDF, electrospinning is a single-step method and is most effective to induce polar phases. [12] Therefore, the electrospinning method is adopted for the fabrication of composite material. Simultaneous use of high field and stretching used in the electrospinning technique induce and enhance the polar phases in PVDF [9, 13, 14]. Furthermore, the electrospun fibers provide a better surface-to-volume ratio, higher

flexibility, and encapsulation property. This makes electrospun fibers useful in a broad range of applications, including catalysis, energy harvesting, tissue engineering, wound healing, filtration membranes, etc. They can be easily engineered upon target applications, which makes them more acceptable. [15, 16]

Composites formed by combining organic and inorganic materials can exhibit the advantages of both constituents and exhibit superior functionalities compared to individuals. PVDF and its copolymers are widely used as the ferroelectric organic counterparts in flexible magnetoelectric multiferroic composites [17–19]. Magnetostrictive particles can be introduced to the polymer to induce magnetoelectric coupling [20, 21]. Dielectric, piezoelectric and mechanical properties can be modified by adding various metal oxides [22–24]. Magnetoelectric materials formed by combining ferroelectric polymers and highly magnetostrictive nanoparticles are gaining considerable attention nowadays. They are potential candidates for flexible electronic device fabrication including sensors, energy harvesters, memory devices recording media, etc. [25–27]

Strontium ferrite $\text{SrFe}_{12}\text{O}_{19}$ (SFO) is a synthetic magnetic material, similar to the magneto-plumbite structure, also known as M-type hexagonal ferrite with space group (P63/mmc) in which spinel ($S = \text{Fe}_6\text{O}_8^{2+}$) and hexagonal ($R = \text{MFe}_6\text{O}_{11}^{2-}$) layers are stacked alternatively [28, 29]. The M-type hexagonal ferrites have emerged as a suitable substitute for rare-earth-based permanent magnets [30]. SFO possess good chemical and thermal stability, high curie temperature, and magnetization [28, 29, 31]. Obrados et al. reported the detailed crystal structure of $\text{SrFe}_{12}\text{O}_{19}$ [32]. The magnetic and structural properties of the SFO nanoparticles derived by the co-precipitation method were reported by Z.F. Zi et al. [29]. Single-phase SFO shows regular hexagonal platelets structure, the cell parameters are found to be, $a = 5.8751 \text{ \AA}$ and $c = 23.0395 \text{ \AA}$ and the magnetic saturation marked 55.73 emu/g at room temperature [29]. Reports on the SFO-incorporated PVDF composite structures and its effects on electroactive phases of PVDF are very few. The effectiveness of PVDF-SFO composite films on the reduction of electromagnetic waves has been reported by S Sutradhar et al. [33]. It shows an excellent microwave absorption around -109.9 dB at 8.5 GHz . The efficiency of SFO fiber-loaded composite films of PVDF-HFP in

the energy storage application has been studied by S. Prathipkumar et al. [34]. SFO nanofibers calcined at $800 \text{ }^\circ\text{C}$ possessed a magnetic saturation above 65 emu/g . The average crystallite size and magnetic saturation are increased with an increase in calcination temperature. The energy storage capacity of the composite films has been improved after the addition of SFO and energy storage of 1750 mJ/cm^3 at 444 kV/cm [34]. SFO holds high coercivity, higher curie temperature ($\approx 463 \text{ }^\circ\text{C}$), and higher dielectric properties, which is also a non-toxic material that finds applications in various fields, including recording media, catalysis, microwave devices, EMI shielding, biosensor, and in applications which makes use of permanent magnets [28, 33, 35–38].

In this work, highly magnetostrictive SFO nanoparticles with different weight percentages (4, 8, 16 wt %) were embedded into the PVDF-HFP fibers to fabricate 0–1 connectivity multiferroic heterostructure. The structural, morphological, dielectric, ferroelectric, and magnetoelectric properties of the composite fiber mats have been investigated.

Experimental

Synthesis of SFO nanoparticles

The sol–gel method was used to synthesize SFO nanoparticles. Strontium nitrate and ferric nitrate were used as the precursors. Precursor solutions were taken individually in deionized water and subjected to ultrasonication for 30 min. When the precursors were dissolved entirely, the solutions were mixed, and polyvinyl alcohol (PVA), which acts as a chelating agent, was added to the mixture. The amount of PVA is fixed as the amount of metal ions in the precursor solution. Then, the mixed solution is kept under stirring at a temperature of $60 \text{ }^\circ\text{C}$ until it forms a brownish gel. The obtained gel is transferred and kept in an oven for 12 h at $120 \text{ }^\circ\text{C}$ to complete the drying process. Then the dried gel was calcined at $800 \text{ }^\circ\text{C}$ for 3 h to obtain SFO nanoparticles.

Preparation of electrospun fibers of PVDF-HFP/SFO

Composite fiber mats were prepared in the following manner. Initially, 15 wt% of PVDF-HFP (Sigma-

Aldrich, average molecular weight (M_w) \approx 455,000) was dissolved in a mixture of solvents, dimethylformamide (DMF), and acetone has taken in the ratio 1:1. When the pellets are completely dissolved SFO nanoparticles were added to the polymer solution. SFO weight percentages (wt%) varied as 4, 8, 16 of the polymer. Then, the composite solution was kept under stirring for 12 h at 60 °C followed by sonication for 2 h. Composite polymer solutions were transferred into a 10 ml syringe. A 15 kV high voltage and 1 ml/hr flow rate were used for the electrospinning technique. More details regarding the spinning parameters used for fabricating PVDF-based composite fiber mats find elsewhere [17]. The prepared samples were labeled PS-4, PS-8, and PS-16 according to their loading content. A schematical

diagram of the preparation of SFO nanoparticles and composite electrospun fiber is shown in Fig. 1a, b.

Characterization

X-Ray diffraction (XRD) patterns of the synthesized nanoparticles, PVDF-HFP pellet, and the composite electrospun samples were made by Rigaku mini flex diffractometer operated at 40 kV and 15 mA with Cu-K α line (wavelength 1.54 Å). XRD data were recorded over a range of 2θ from 10° to 80°. Characteristics vibrational modes present in the polymer samples were detected by PerkinElmer Spectrum 400 spectrometer. TEM images of the samples were obtained using JEOL JEM 2100 transmission electron microscope operated at 200 kV equipped with a Lanthanum Hexa boride (LaB₆) lamp for bright field

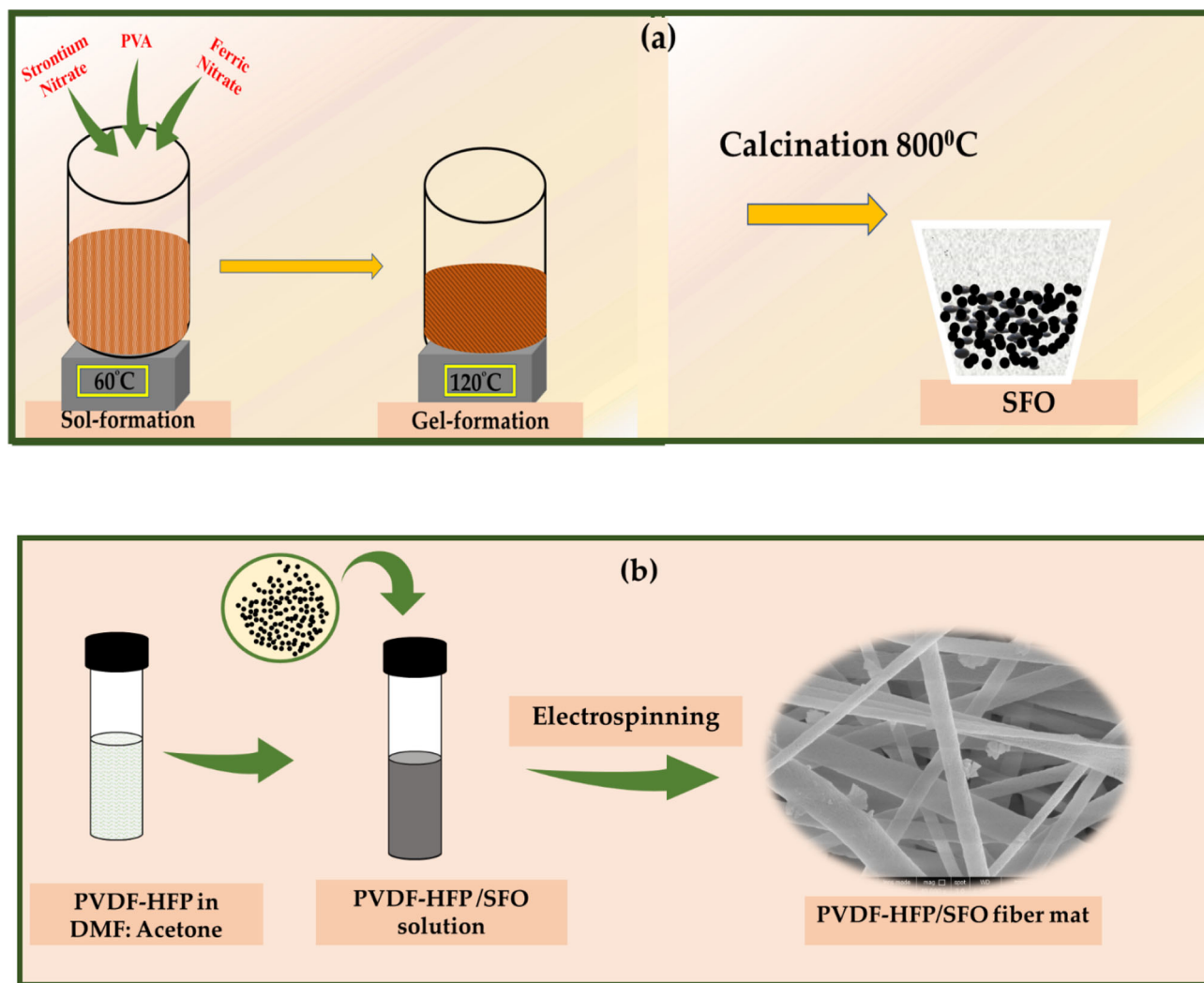


Figure 1 a Graphical representation of the preparation of SFO nanoparticles and b PVDF-HFP/SFO composite fiber mat.

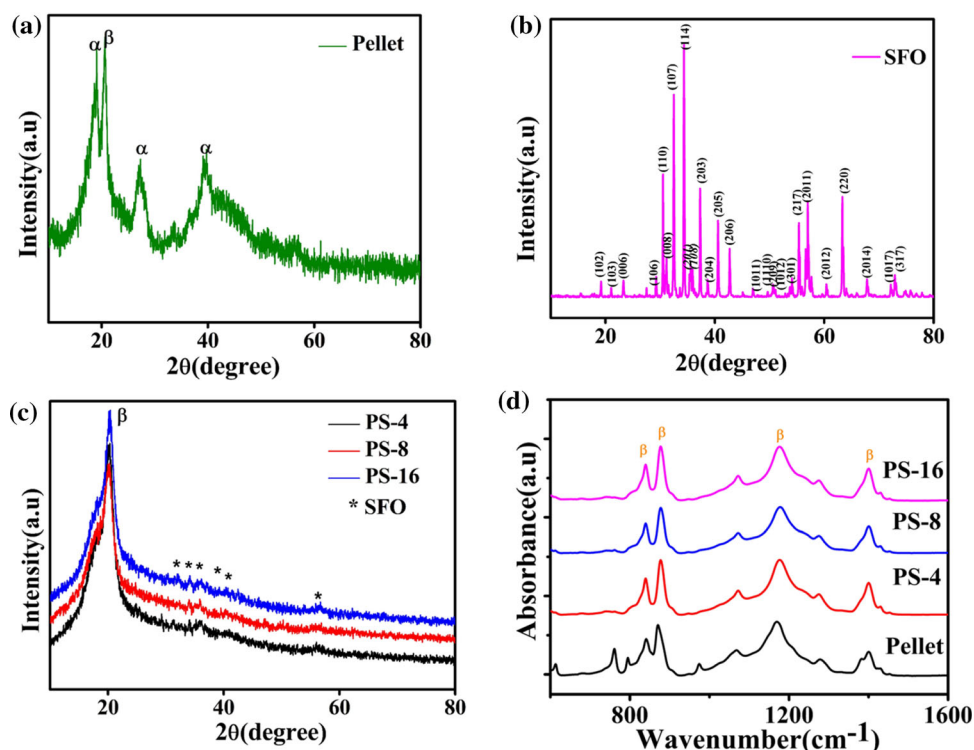
imaging. Elemental analysis has been carried out by an Oxford EDAX system attached to the TEM instrument. FESEM images were also taken using NOVA Nano SEM 450 to characterize the morphology of the electrospun samples fabricated. Secondary electron (SE) mode with a high voltage of 10 kV is used to obtain high-resolution images. Dielectric properties were measured by an Agilent E4980A precision LCR meter in a range of 500 Hz–2 MHz at room temperature. The P-E loop tracer purchased from Marine India was used to perform the P-E loop measurements at room temperature. Magnetoelectric coupling voltage was measured using a lock-in amplifier ME setup. Mechanical properties of the pure and composite fiber mats were done using Universal Testing Machine (UTM) Tinius Olsen H25KL (ASTM D 882-12). Gauge separation of 40 mm, a speed of 5.00 mm/min, and 100 Newton load cells were used to study the mechanical properties of the fiber mats.

Result and discussion

Structural characterizations

The X-ray diffraction technique (XRD) investigates the crystallinity of the prepared inorganic filler and filler-loaded PVDF-HFP electrospun nanocomposite fibers. Figure 2a represents the X-ray diffraction pattern of the PVDF-HFP pellet. Peaks corresponding to the non-polar α phase are detected along with the polar β phase and marked in Fig. 2a. Peaks observed at 18.8, 27.2, and 39.5° are attributed to the non-polar crystalline phase α in the polymer PVDF-HFP [39–41]. The peak detected at 20.6° (110/200) is a characteristic peak of the ferroelectric β phase [39, 40]. Characteristic reflection planes, the structure purity, and the average particle size of the prepared SFO nanoparticles have been analyzed from the XRD pattern of SFO, shown in Fig. 2b and the respective planes of SFO are indexed according to JCPDS card No: 79–1412. The average crystallite size of the SFO nanoparticles has been calculated from the Scherrer equation and found to be 53 nm. XRD patterns of nanocomposite electrospun fibers are shown in Fig. 2c. It is observed that the peaks representing the non-polar α are reduced, and some peaks are completely disappeared. The peak at $2\theta = 20.2^\circ$

Figure 2 XRD spectrum of **a** PVDF-HFP pellet **b** SFO nanoparticles **c** PS-4, PS-8 and PS-16 composite electrospun samples. **d** FTIR spectrum of PVDF-HFP pellet, PS-4, PS-8 and PS-16 composite electrospun samples.



representing the plane (110/200) which corresponds to the β phase, is the only peak that arises from the polymer fibers in the composite structure [39]. The vanishing of peaks related to the α phase in the composite validates the influence of SFO and the electrospinning technique in promoting the electroactive β phase in PVDF-HFP. It has been noted that the characteristic peaks of hexagonal SFO are visible in the XRD patterns of composite fiber mats and marked as * in Fig. 2c. Thus, the successful loading of SFO nanoparticles in the polymer fiber mat is confirmed and the peaks resulting from the SFO are indexed in the XRD pattern of the composite. The resultant peak intensifies with the increasing filler loading.

The Crystallite size of the β phase observed in the composite fiber samples and the PVDF-HFP pellet was calculated using the Scherrer equation

$$D = \frac{K\lambda}{(\beta \cos \theta)} \quad (1)$$

where K is the constant ≈ 0.9 , λ is the wavelength used which is $\approx 1.54 \text{ \AA}$, β is the Full width half maximum (FWHM), and θ is the diffraction angle. The crystallite size of the ferroelectric β phase in the Pellet structure is found to be = 15 nm. However, the crystallite size of the β phase in the composite fiber samples is found to be = 5 nm and 6 nm. A detailed study on the crystallite size and its effect on dipole orientation in PVDF and its copolymers are reported by F. Guan et al [42].

In order to get a better understanding of the structural transformation that occurred in the various crystalline phases, FTIR analysis has also been done. FTIR spectra of the PVDF-HFP pellet and PVDF-HFP/SFO with various filler loadings are given in Fig. 2d. As shown in Fig. 2d the PVDF-HFP pellet sample is in the heterophase; the characteristic absorption bands of both non-polar α and polar β phases are detected in the PVDF-HFP pellet sample. The peaks indexed in the range of 610 (CF_2 wagging), 760 (CF_2 bending), 795 (CH_2 rocking) and 976 (CH_2 out of plane deformation) cm^{-1} are attributed to the non-polar α phase. Meanwhile, the bands observed at 839 (CH_2 rocking, CF_2 stretching), 878 (combined CF_2 and C–C stretching), 1176 (symmetrical stretching mode CF_2), and 1400 (bending or scissoring of CH_2) cm^{-1} are the characteristic vibrational bands of β phase [17, 43, 44]. FTIR spectra showed that the non-polar α phase has diminished, and the intensity of the

peaks attributed to the polar β phase is noticeably enhanced.

Both the XRD and FTIR result confirms the polar β phase-chain confirmation in all-trans configuration as the significant phase present in the prepared electrospun fiber mat systems. During the electrospinning process, axial stretching and high voltage act together to achieve the maximum polar phase [45]. Coulombic interaction originated due to the high field results in the thinning and bending of the jet formed during the spinning process [16]. The stretching process causes the orientation of the dipoles in the same direction, transformation to the most ferroelectric $-\beta$ phase, which is a result of the all-trans chain configuration [45].

Morphological characterizations

To study morphology and the effect of the inorganic filler in the nanofiber structure, FESEM images have been taken. Figure 3a, b shows the FESEM images of PVDF-HFP pure mat and PS-8 samples. The images clearly show the beadless-defect-free fibers. In the FESEM images of the PS-8 samples, the added SFO nanoparticles are visible and are attached to the surface of the polymer fiber. Hence, the FESEM images show the distribution of SFO nanoparticles on the polymer fibers.

TEM images of the composite fiber sample PS-16 are shown in Fig. 4a, b. The successful loading of the SFO nanoparticles in the polymer system is observed from the TEM images. SAED pattern of the same shown in Fig. 4c confirms the crystalline nature of the sample. Energy dispersive elemental spectroscopy (EDAX) determines the elemental composition and confirms the presence of required elements in the sample. EDAX spectrum shown in Fig. 5 validates the presence of Strontium, Iron, Fluorine, Oxygen in the prepared sample.

Dielectric and Ferroelectric properties

Dielectric properties of the PVDF-HFP mat and PVDF-HFP/SFO nanocomposite mats were investigated in terms of their frequency dependence (500 Hz–2 MHz) at room temperature. Figure 6a–c illustrates the Frequency-dependent dielectric properties such as the dielectric constant (ϵ'), and dielectric loss (ϵ''). The results showed that the dielectric constant significantly increased with the increase in

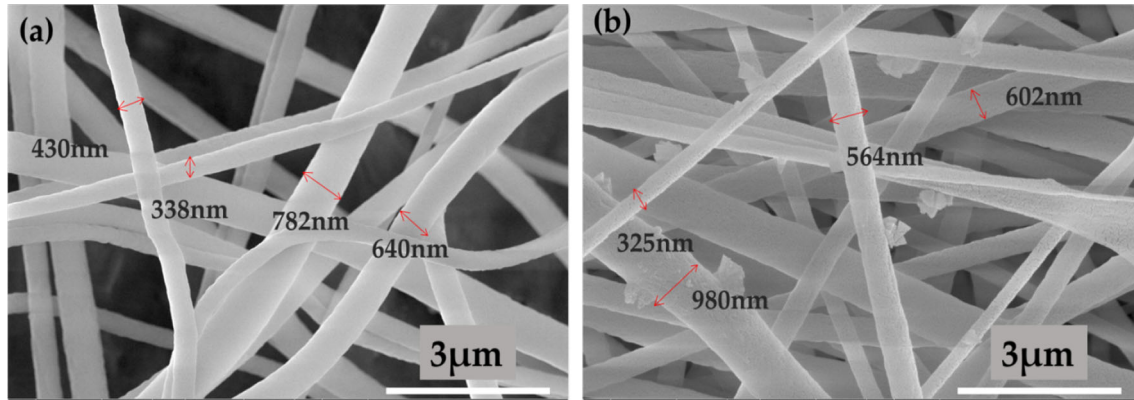


Figure 3 FESEM images of **a** pure PVDF-HFP and **b** PS-8 composite electrospun samples.

Figure 4 **a, b** TEM images and **c** SAED pattern of PS-16 composite electrospun samples.

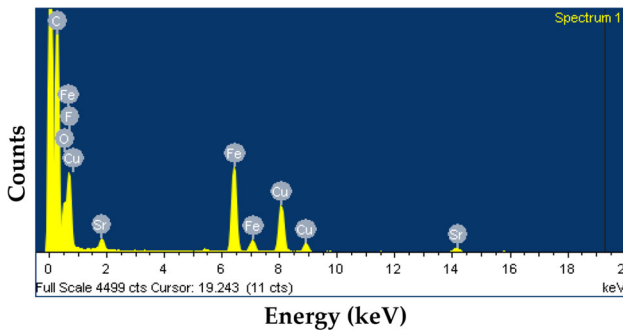
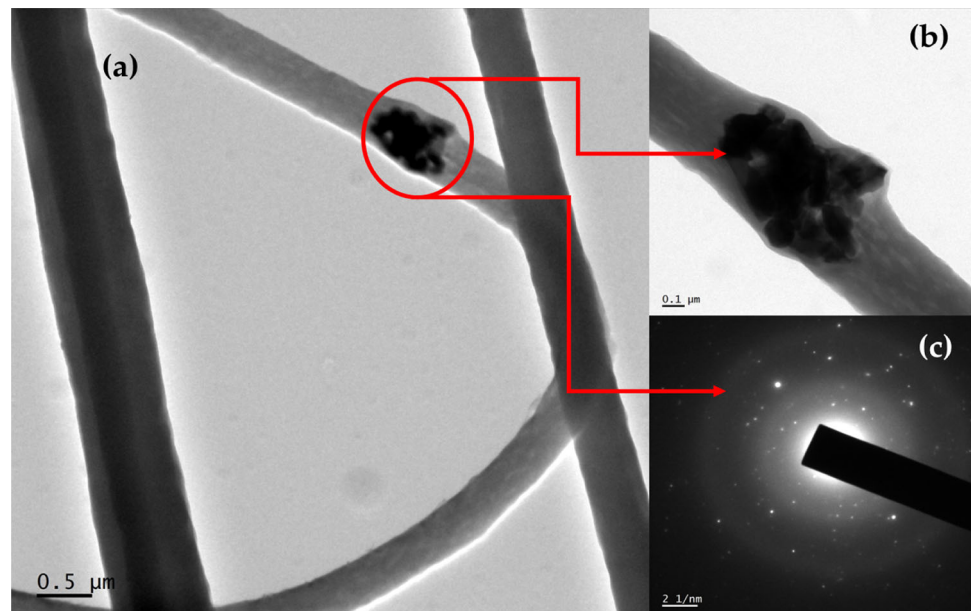
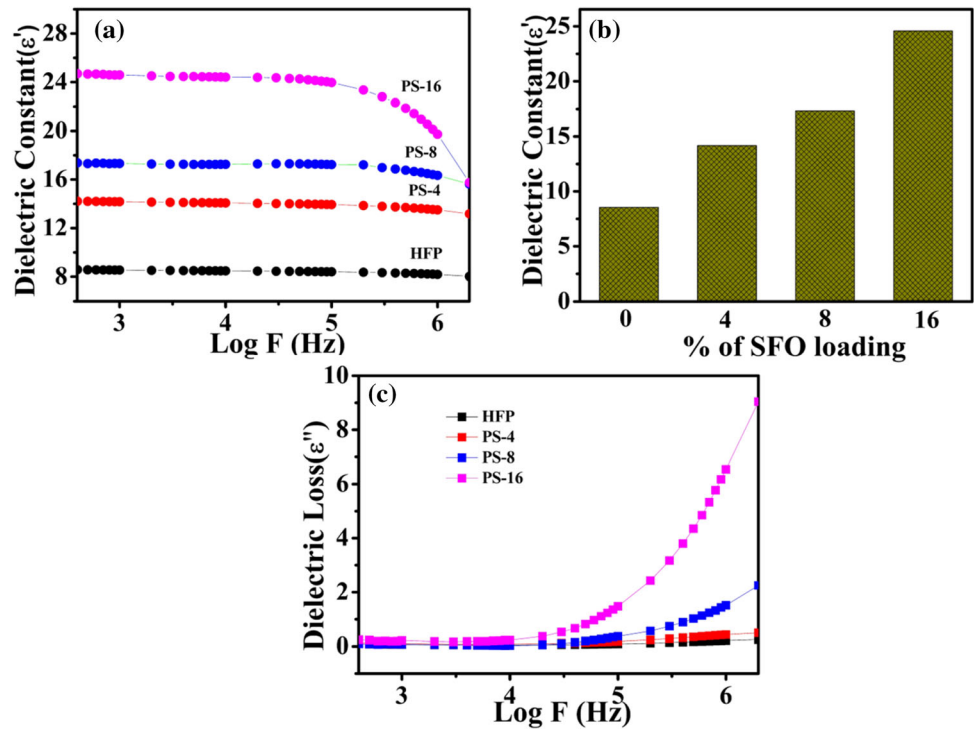


Figure 5 EDAX spectrum of PS-16 composite sample.

inorganic filler concentration. Similar reports have been obtained in various ferrite-loaded PVDF composites [17, 18, 46, 47]. However, the dielectric constant remains almost in a steady state in a wide range

of frequencies and shows a tendency to decrease after 1 MHz. Figure 6b shows the dielectric constant value of the PVDF-HFP fiber mat (abbreviated as HFP), PVDF-HFP/SFO with various filler loadings at 1 kHz. To better explain the process of higher dielectric constant in the low-frequency region, and the reduction in the high-frequency region, the Maxwell–Wagner–Sillars polarization effect can be used. When the frequency increases, the dipoles were unable to follow the rapid frequency variation happening in the AC field, so the resultant polarization becomes small in higher frequencies [48–50]. Notably, the dielectric constant of 16 wt% SFO loaded composite sample is increased by about 25 at 1 kHz, which is remarkably higher than that of the pure HFP system. As the filler concentration increases, the

Figure 6 **a** Frequency dependence of dielectric constant of PVDF-HFP PS-4, PS-8 and PS-16 samples at room temperature. **b** Dielectric constant at 1 kHz with filler loading **c** Dielectric loss (ϵ'') of PVDF-HFP, PS-4, PS-8 and PS-16 samples.



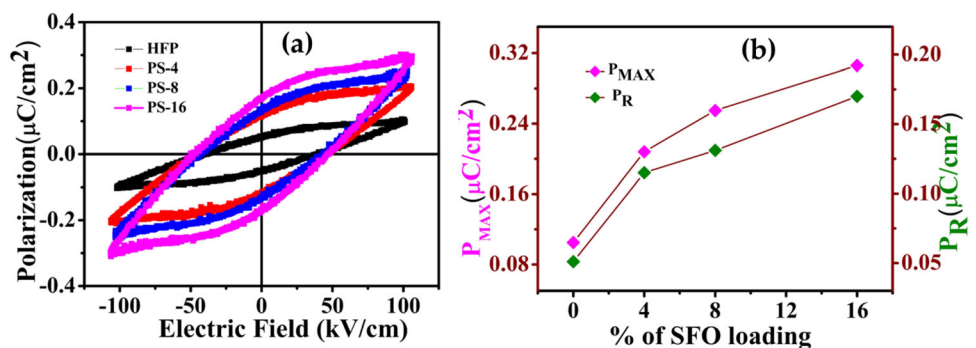
interfacial area between the organic and inorganic components increases, and it will improve the interfacial polarizations and the dielectric constant [17, 24].

Variations in dielectric loss (ϵ'') with Log F are illustrated in Fig. 6c. From Fig. 6c, it is clear that the loss values are increased with an increase in inorganic filler loading. The dielectric loss was marked very small for the prepared nanocomposite samples at lower frequencies. Though it is small for lower frequency regions a sharp increase is observed at higher frequencies. A similar trend in dielectric loss/tangent loss factor was reported in PVDF-based nanocomposites [24, 51].

Polarization-Electric field (P-E) hysteresis loops are used to study the ferroelectric properties of the

prepared electrospun fiber mats. We have performed the room temperature P-E hysteresis loop measurements of the PVDF-HFP mat and the PVDF-SFO-loaded composite fiber mats, which were taken at 50 Hz. Figure 7a illustrates the P-E loops of the PVDF-HFP mat and PVDF-HFP/SFO mat with a varying load of SFO (4, 8, 16 wt%). The P-E loops associated with all the samples are analyzed and the changes observed in the maximum polarization (P_{max}) and remnant polarization (P_R) values with the filler loading are plotted in Fig. 7b. It is noted that the ferroelectric parameters such as P_{max} and P_R of the composites are improved with an increase in the inorganic filler loading, which supports the facts that Hexa ferrite-SFO acts as a nucleating agent in enhancing electroactivity in the PVDF-HFP [34]. As a

Figure 7 **a** P-E loops were obtained for PVDF-HFP, PS-4, PS-8 and PS-16 samples **b** changes in the ferroelectric parameters with filler loading.



result, higher filler loading results in higher P_{\max} and P_R . This may be due to the increase in interfacial area between the nanoparticles and the polymer [52].

Magnetolectric studies

Magnetolectric coupling in composite multiferroic materials is a product tensor property. It evolves indirectly through the spin exchange, or stress/strain-mediated mechanism [6]. Among the various mechanisms, stress- or strain-mediated interactions have been explored intensively. There must be at least two phases (magnetostrictive and piezoelectric) in the hybrid system to exhibit magnetolectric properties [2, 6, 53]. In most polymer-based magnetolectric materials, the magnetostrictive phase is provided by ferrites and, PVDF and its copolymers give the ferroelectric phase. Magnetostrictive inorganic nanoparticles SFO, in the piezoelectric PVDF-HFP-fibers result in a cross-coupling between magnetic and electric orderings in the resultant polymer nanocomposite system. An ME voltage is induced in the composite samples by applying a DC bias field of 1kOe. Magnetolectric coupling voltage, originated in the organic–inorganic composite fiber structure is measured using an ME lock-in amplifier setup. The ME-induced voltage plotted against AC magnetic field is shown in Fig. 8a and the induced ME voltage shows a linear dependence on the applied field. An increase in the magnetostrictive filler concentration, increased the induced ME voltage.

The magnetolectric coupling coefficient (MECC), the figure of merit of the magnetolectric property, can be calculated from equation, [54]

$$\alpha_{\text{ME}} = \left(\frac{V}{H \times t} \right) \quad (2)$$

where V is the induced ME voltage, t is the thickness of the sample, and H is the AC field. MECC values of the prepared nanocomposite samples are shown in Fig. 8b. Following the same trend of the ME voltage, MECC also increases with filler loading. For an amount of 4 wt% of inorganic SFO-filler loading, MECC marked a significant value of 14.7 mV/cm.Oe, which is quite remarkable for such a lower filler content. Additional filler content increased the MECC and reached a maximum of 19.9 mV/cm.Oe for 16 wt% of SFO. It has been reported that in stress- or strain-mediated composite ME materials, the ME property originates in the interfaces, and the successful loading of the inorganic magnetostrictive filler increases the resultant interfacial area [55]. This will allow more effective strain transfer through the polymer matrix.

Mechanical characterization

Mechanical characterizations were also done to study the tensile properties of the polymer multiferroic fibers. ASTM D 882-12 with the conditions; of gauge separation of 40 mm and a test speed of 5.00 mm/min were used to study the mechanical properties of the fiber mats. Stress-Strain graphs obtained for PVDF-HFP pure sample mat, PS-4 and PS-16 samples are plotted in Fig. 9a. The observed Young's modulus and Tensile strength values are shown in Fig. 9b. From Fig. 9b, it can be seen that the addition of inorganic filler modified the tensile properties of the polymer slightly. For lower filler content the tensile parameters declined a little and the further increase in the filler content slightly improved the mechanical properties of the composite.

Figure 8 a Magnetolectric Voltage with applied AC field b MECC achieved for different filler loading.

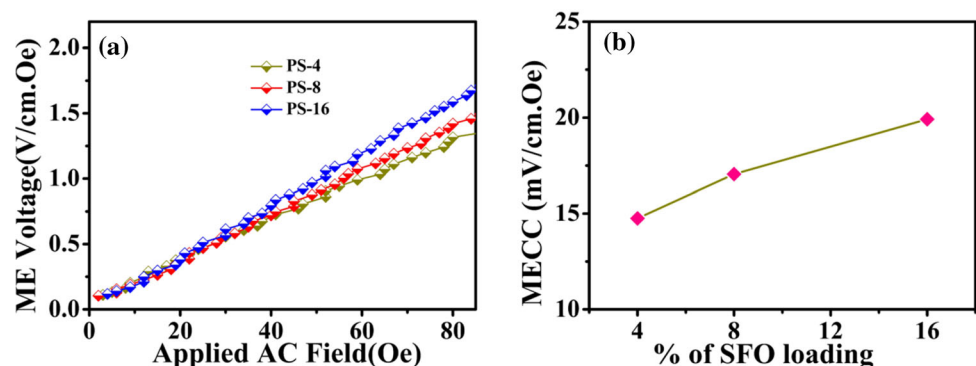
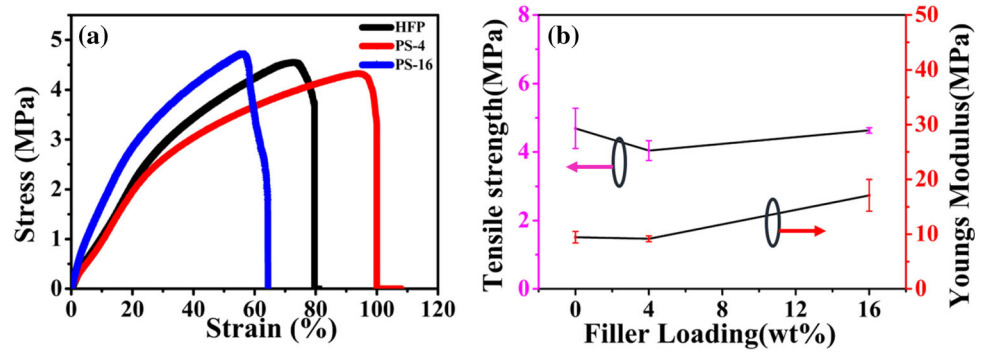


Figure 9 a Stress–Strain Graph b Tensile strength (MPa) and Young’s Modulus (MPa) obtained for PVDF-HFP pure, PS-4 and PS-16 fiber mats.



Conclusion

SrFe₁₂O₁₉ (SFO)-loaded PVDF-HFP multiferroic nanocomposite fibers were successfully fabricated by an electrospinning technique. Enhancement in the electroactive phase of the PVDF-HFP has been confirmed using XRD and FTIR techniques. The prepared PVDF-HFP/SFO systems exhibited remarkable multiferroic traits. The dielectric constant value of the highest filler-loaded system reached 25 at 1 kHz. Ferroelectric properties of the hybrid system have been studied using a P-E loop measurement system and the values of P_{\max} and P_R were enhanced with SFO loading. To confirm the existence of magneto-electric coupling in the fabricated system, the MECC value of the magneto-electric fibers has also been calculated and marked 19.9 mV/cm. Oe for 16 wt % filler loading. The remarkable MECC, dielectric properties, and flexibility make it a potential candidate in flexible device fabrication including energy storage, and data storage devices.

Acknowledgements

The corresponding author B.R, acknowledges the financial support received from MoE Govt. of India through the STARS project (MoE-STARS/STARS1/443). Authors S.K.C and B.R are thankful to Prof.Dr.Nandakumar Kalarikkal for providing Dielectric and Magneto-electric coupling measurement facility. The authors wish to thank Prof.Dr.Sabu Thomas for extending the UTM facility. S.K.C and B.R also acknowledge the help of Mr.Rahul M.T., Mr. Karthik Vinodan, and Ms. Milanta Tom for the dielectric, ferroelectric and UTM studies.

References

- [1] Bichurin M, Petrov V, Priya S, Bhalla A (2012) Multiferroic magneto-electric composites and their applications. *Adv Condens Matter Phys*
- [2] Nan CW, Bichurin MI, Dong S, Viehland D, Srinivasan G (2008) Multiferroic magneto-electric composites: historical perspective, status, and future directions. *J Appl Phys* 103(3):1
- [3] Wang Y, Hu J, Lin Y, Nan CW (2010) Multiferroic magneto-electric composite nanostructures. *NPG Asia Mater* 2:61–68
- [4] Vopson MM (2015) Fundamentals of multiferroic materials and their possible applications. *Crit Rev Solid State Mater Sci* 40(4):223–250
- [5] Gupta R, Kotnala RK (2022) A review on current status and mechanisms of room-temperature magneto-electric coupling in multiferroics for device applications. *J Mater Sci* 57:12710–12737
- [6] Pradhan DK, Kumari S, Rack PD (2020) Magneto-electric composites: applications, coupling mechanisms, and future directions. *Nanomaterials* 10(10):2072
- [7] Martins P, Lanceros-Méndez S (2013) Polymer-based magneto-electric materials. *Adv Funct Mater* 23:3371–3385
- [8] Zhang QM, Bharti V, Kavarnos G (2002) Poly(vinylidene fluoride) (PVDF) and its copolymers. In: Schwartz M (ed) *Encyclopedia of smart materials*. <https://doi.org/10.1002/0471216275.esm063>
- [9] Martins P, Lopes A, Mendez SL (2014) Electroactive phases of poly (vinylidene fluoride): determination processing and applications. *Prog Polym Sci* 39(4):683–706
- [10] Jiang B, Wei Y, Wu J, Cheng H, Yuan L, Li Z, Xu H, Huang Y (2021) Recent progress of asymmetric solid-state electrolytes for lithium/sodium-metal batteries. *EnergyChem* 3(5):100058

- [11] Ruan L, Yao X, Chang Y, Zhou L, Qin G, Zhang X (2018) Properties and applications of the β phase poly (vinylidene fluoride). *Polymers* 10(3):228
- [12] He Z, Rault F, Lewandowski M, Mohsenzadeh E, Salaün F (2021) Electrospun PVDF nanofibers for piezoelectric applications: a review of the influence of electrospinning parameters on the β phase and crystallinity enhancement. *Polymers* 13:1–23
- [13] Mokhtari F, Latifi M, Shamshirsaz M (2015) Electrospinning/electrospray of polyvinylidene fluoride (PVDF): piezoelectric nanofibers. *J Text Inst* 107:1–19
- [14] Szweczyk PK, Gradys A, Kim SK, Persano L, Marzec M, Krysztal A, Busolo T, Toncelli A, Pisignano D, Bernasik A, Kar-Narayan S, Sajkiewicz P, Stachewicz U (2020) Enhanced piezoelectricity of electrospun polyvinylidene fluoride fibers for energy harvesting. *ACS Appl Mater Interfaces* 12:13575–13583
- [15] Xue J, Wu T, Dai Y, Xia Y (2019) Electrospinning and electrospun nanofibers: methods, materials, and applications. *Chem Rev* 119(8):5298–5415
- [16] Greiner A, Wendorff JH (2007) Electrospinning: a fascinating method for the preparation of ultrathin fibers. *Angew Chem Int Ed* 46:5670–5703
- [17] Chacko SK, Rahul MT, Raneesh B, Kalarikkal N (2020) Enhanced magnetoelectric coupling and dielectric constant in flexible ternary composite electrospun fibers of PVDF-HFP loaded with nanoclay and NiFe_2O_4 nanoparticles. *New J Chem* 44(26):11356–11364. <https://doi.org/10.1039/d0nj02494e>
- [18] Rahul MT, Chacko SK, Raneesh B, Nambissan PMG, Kalarikkal N, Thomas S (2022) $\text{Al}_3\text{Fe}_5\text{O}_{12}$ nanoparticles loaded electrospun PVDF fibres: an inorganic-organic material with multifunctional traits. *Mater Chem Phys* 282:125977
- [19] Rahul MT, Chacko SK, Raneesh B, Philip KA, Kalarikkal N, Rouxel D, Munirathinam P, Chandrasekhar A (2022) Hydrated metal salt and $\text{Y}_3\text{Fe}_5\text{O}_{12}\text{-Na}_0.5\text{K}_0.5\text{NbO}_3$ -incorporated P(VDF-HFP) films: a promising combination of materials with multiferroic and energy harvesting properties. *J Mater Sci* 57:7653–7666. <https://doi.org/10.1007/s10853-022-07142-7>
- [20] Rahul MT, Chacko SK, Vinodan K, Raneesh B, Bhadrappriya BC, Bose BA, Kalarikkal N, Rouxel D, Viswanathan P, Chandrasekhar A (2022) Multiferroic and energy harvesting characteristics of P (VDF-TrFE)- CuFe_2O_4 flexible films. *Polymer* 252:124910
- [21] Prathipkumar S, Hemalatha J (2020) Magnetoelectric response and tunneling magnetoresistance behavior of flexible P(VDF-H FP)/cobalt ferrite nanofiber composite films. *Ceram Int* 46:258–269
- [22] Parangusan H, Ponnamma D, Al-Maadeed MAA (2018) Stretchable electrospun PVDF-HFP/Co-ZnO nanofibers as piezoelectric nanogenerators. *Sci Rep* 8(1):1–11
- [23] Mayeen A, Kala MS, Sunija S, Rouxel D, Bhowmik RN, Thomas S, Kalarikkal N (2020) Flexible dopamine-functionalized $\text{BaTiO}_3/\text{BaTiZrO}_3/\text{BaZrO}_3$ -PVDF ferroelectric nanofibers for electrical energy storage. *J Alloys Compd* 837:155492
- [24] Mayeen A, Kala MS, Jayalakshmy MS, Thomas S, Philip J, Rouxel D, Bhowmik RN, Kalarikkal N (2019) Flexible and self-standing nickel ferrite-PVDF-TrFE cast films: promising candidates for high-end magnetoelectric applications. *Dalton Trans* 48:16961–16973
- [25] Chacko SK, Rahul MT, Balakrishnan R (2022) Magnetoelectric polymer nanocomposites for energy harvesting. In: Balakrishnan R (ed) Sobi K Chacko, MT Rahul. Elsevier, Engineered polymer nanocomposites for energy harvesting applications, pp 203–224
- [26] Gonçalves R, Larrea A, Sebastian MS, Sebastian V, Martins P, Lanceros-Mendez S (2016) Synthesis and size dependent magnetostrictive response of ferrite nanoparticles and their application in magnetoelectric polymer-based multiferroic sensors. *J Mater Chem C Mater* 4:10701–10706
- [27] Ahlawat A, Satapathy S, Shirolkar MM, Li J, Khan AA, Deshmukh P, Wang H, Choudhary RJ, Karnal AK (2018) Tunable magnetoelectric nonvolatile memory devices based on $\text{SmFeO}_3/\text{P(VDF-TrFE)}$ nanocomposite films. *ACS Appl Nano Mater* 1:3196–3203
- [28] Stingaciu M, Topole M, McGuinness P, Christensen M (2015) Magnetic properties of ball-milled $\text{SrFe}_{12}\text{O}_{19}$ particles consolidated by spark-plasma sintering. *Sci Rep* 5:1–8
- [29] Zi ZF, Sun YP, Zhu XB, Yang ZR, Dai JM, Song WH (2008) Structural and magnetic properties of $\text{SrFe}_{12}\text{O}_{19}$ hexaferrite synthesized by a modified chemical co-precipitation method. *J Magn Magn Mater* 320:2746–2751
- [30] de Julián Fernández C, Sangregorio C, de la Figuera J, Belec B, Makovec D, Quesada A (2021) Progress and prospects of hard hexaferrites for permanent magnet applications. *J Phys D Appl Phys* 54(15):153001
- [31] Yongfei W, Qiaoling L, Cunrui Z, Hongxia J (2009) Preparation and magnetic properties of different morphology nano- $\text{SrFe}_{12}\text{O}_{19}$ particles prepared by sol-gel method. *J Alloys Compd* 467:284–287

- [32] Obradors X, Solans X, Collomb A, Samaras D, Rodriguez J, Pernet M, Font-Altaba M (1988) Crystal structure of strontium hexaferrite $\text{SrFe}_{12}\text{O}_{19}$. *J Solid State Chem* 72:218–224
- [33] Sutradhar S, Saha P, Chowdhury A, Das S (2019) Reduction of electromagnetic pollution by the enhancement of microwave absorption of strontium hexaferrite functionalized poly(vinylidene fluoride) composite film. *Mater Res Express* 6(8):086424
- [34] Prathipkumar S, Hemalatha J (2022) Magnetoelectric behavior and magnetic field-tuned energy storage capacity of $\text{SrFe}_{12}\text{O}_{19}$ nanofiber reinforced P (VDF-HFP) composite films. *J Magn Magn Mater* 555:169378
- [35] Acharya S, Gopinath CS, Alegaonkar P, Datar S (2018) Enhanced microwave absorption property of reduced graphene oxide (RGO)–strontium hexaferrite (SF)/poly(vinylidene fluoride) (PVDF). *Diam Relat Mater* 89:28–34
- [36] Safronov AP, Mikhnevich EA, Lotfollahi Z, Blyakhman FA, Sklyar TF, Larrañaga Varga A, Medvedev AI, Fernández Armas S, Kurlyandskaya GV (2018) Polyacrylamide ferrogels with magnetite or strontium hexaferrite: next step in the development of soft biomimetic matter for biosensor applications. *Sensors* 18(1):257
- [37] Rashid AU, Southern P, Darr JA, Awan S, Manzoor S (2013) Strontium hexaferrite ($\text{SrFe}_{12}\text{O}_{19}$) based composites for hyperthermia applications. *J Magn Magn Mater* 344:134–139
- [38] Shirsath SE, Kadam RH, Batoo KM, Wang D, Li S (2020) Co–Al-substituted strontium hexaferrite for rare earth free permanent magnet and microwave absorber application. *J Phys D Appl Phys* 54(2):024001
- [39] Tawansi A, Oraby AH, Abdelrazek EM, Abdelaziz M (1999) Structural and electrical properties of MgCl_2 -filled PVDF films. *Polym Test* 18:569–579
- [40] Abdullah IY, Yahaya M, Jumali MHH, Shanshool HM (2014) Effect of annealing process on the phase formation in poly(vinylidene fluoride) thin films. *AIP Conf Proc* 1614:147–151
- [41] Chacko SK, Rahul MT, Raneesh B, Vinodan K, Jose JK, Kalarikkal N (2022) Enhanced electroactive phase, dielectric properties and tuning of bandgap in Ho^{3+} modified PVDF-HFP composite films. *J Polym Res* 29(11):1–10. <https://doi.org/10.1007/S10965-022-03318-6>
- [42] Guan F, Wang J, Pan J, Wang Q, Zhu L (2010) Effects of polymorphism and crystallite size on dipole reorientation in poly(vinylidene fluoride) and its random copolymers. *Macromolecules* 43:6739–6748
- [43] Sousa RE, Nunes-Pereira J, Ferreira JCC, Costa CM, Machado AV, Silva MM, Lanceros-Mendez S (2014) Microstructural variations of poly(vinylidene fluoride co-hexafluoropropylene) and their influence on the thermal, dielectric and piezoelectric properties. *Polym Test* 40:245–255
- [44] Divya S, Shakthi T, Hemalatha J (2016) Synthesis and ferroelectric investigations of poly(vinylidene fluoride-co-hexafluoropropylene)-Mg (NO_3)₂ films. *J Appl Polym Sci* 133(40)
- [45] Ribeiro C, Sencadas V, Ribelles JLG, Lanceros-Méndez S (2010) Influence of processing conditions on polymorphism and nanofiber morphology of electroactive poly(vinylidene fluoride) electrospun membranes. *Soft Mater* 8:274–287
- [46] Mayeen A, Subair SS, Nair KMS, Thomas S, Kalarikkal N (2020) Morphological and electrical properties of calcium ferrite loaded polyvinylidene fluoride-hexafluoro propylene nanofibers. In: *AIP Conference Proceedings*, November, vol. 2287, no. 1. AIP Publishing LLC, p 020002
- [47] Mayeen A, Kala MS, Jayalakshmy MS, Thomas S, Philip J, Rouxel D, Bhowmik RN, Kalarikkal N (2019) Flexible and self-standing nickel ferrite–PVDF–TrFE cast films: promising candidates for high-end magnetoelectric applications. *Dalton Trans* 48:16961–16973
- [48] Chinya I, Sen S (2017) Improved dielectric and touch sensing performance of surface modified zinc ferrite (ZF)/polyvinylidene fluoride (PVDF) composite. *Sens Actuators A Phys* 267:301–309
- [49] Chaurasiya A, Pal P, Vas JV, Kumar D, Piramanayagam SN, Singh AK, Medwal R, Rawat RS (2020) Nickel ferrite embedded polyvinylidene fluoride composite based flexible magneto-electric systems. *Ceram Int* 46:25873–25880
- [50] Gheorghiu F, Stanculescu R, Curecheriu L, Brunengo E, Stagnaro P, Tiron V, Postolache P, Buscaglia MT, Mitoseriu L (2020) PVDF–ferrite composites with dual magnetopiezoelectric response for flexible electronics applications: synthesis and functional properties. *J Mater Sci* 55:3926–3939
- [51] Wang Q, Zhang J, Zhang Z, Hao Y, Bi K (2020) Enhanced dielectric properties and energy storage density of PVDF nanocomposites by co-loading of BaTiO_3 and CoFe_2O_4 nanoparticles. *Adv Compos Hybrid Mater* 3:58–65
- [52] Rana DK, Singh SK, Kundu SK, Roy S, Angappane S, Basu S (2019) Electrical and room temperature multiferroic properties of polyvinylidene fluoride nanocomposites doped with nickel ferrite nanoparticles. *New J Chem* 43:3128–3138

- [53] Srinivasan G (2010) Magnetolectric composites. *Annu Rev Mater Res* 40:153–178
- [54] Thankachan RM, Raneesh B, Mayeen A, Karthika S, Vivek S, Nair SS, Thomas S, Kalarikkal N (2018) Room temperature magnetolectric coupling effect in CuFe_2O_4 - BaTiO_3 core-shell and nanocomposites. *J Alloys Compd* 731:288–296
- [55] Nan CW (1994) Magnetolectric effect in composites of piezoelectric and piezomagnetic phases. *Phys Rev B* 50(9):6082

Publisher's Note Springer Nature remains neutral with regard to jurisdictional claims in published maps and institutional affiliations.

Springer Nature or its licensor (e.g. a society or other partner) holds exclusive rights to this article under a publishing agreement with the author(s) or other rightsholder(s); author self-archiving of the accepted manuscript version of this article is solely governed by the terms of such publishing agreement and applicable law.